

Fabrication and Characterization of Ozenoxacin and Curcumin Loaded Electrospun Nanofibre Membrane for Full Thickness Wound Healing: *In vitro* Assessments

Vasanth A¹, Subashini P¹, Jerad Suresh A², Mubeena S³, Alan Mathew Punnoose⁴, Saba Maanvizhi^{1,*}

¹Department of Pharmaceutics, Sri Ramachandra Faculty of Pharmacy, Sri Ramachandra Institute of Higher Education and Research (DU), Porur, Chennai, Tamil Nadu, INDIA.

²Department of Pharmaceutical Chemistry, Sri Ramachandra Faculty of Pharmacy, Sri Ramachandra Institute of Higher Education and Research (DU), Porur, Chennai, Tamil Nadu, INDIA.

³Stem Cell and Regenerative Biology Laboratory, Sri Ramachandra Faculty of Clinical Research, Sri Ramachandra Institute of Higher Education and Research (DU), Porur, Chennai, Tamil Nadu, INDIA.

⁴Department of Clinical Research, Sri Ramachandra Faculty of Clinical Research, Sri Ramachandra Institute of Higher Education and Research (DU), Porur, Chennai, Tamil Nadu, INDIA.

Submission Date: 21-10-2024; Revision Date: 16-11-2024; Accepted Date: 19-12-2024.

ABSTRACT

Background: The development of advanced wound care solutions is critical due to the significant global impact of chronic and acute wounds. This study focuses on fabrication of a biodegradable and biocompatible nanofibre scaffold for enhanced wound healing, combining antimicrobial and anti-inflammatory properties. **Objectives:** The present research work was carried out to fabricate and evaluate nanofibres loaded with ozenoxacin (anti-microbial agent) and curcumin (anti-inflammatory agent) for their potential in advanced wound management. **Materials and Methods:** The current study was carried out during December 2023 to July 2024. Nanofibres were developed using electrospinning with a Polyvinyl Alcohol (PVA) and gelatin blend, incorporating with ozenoxacin and curcumin as therapeutic agents. **Results:** The viscosity of the polymer solution prior to electrospinning was found to be at 39.48 Pa.s, ensuring optimal fibre formation. Scanning Electron Microscopy confirmed uniform fibres with diameters between 50-114 nm. Fourier-Transform Infrared Spectroscopy (FT-IR) and X-ray Diffraction (XRD) analyses verified that there is no chemical interaction and further crystalline nature of the incorporated agents respectively. *In vitro* release studies demonstrated a sustained release profile of both ozenoxacin and curcumin over 24 hr, indicating prolonged therapeutic potential. Folding endurance tests revealed that the nanofibres could withstand up to 93 folds without breaking, indicating good mechanical robustness. The study found that ozenoxacin-loaded nanofibers have excellent hydration capacity and drug entrapment efficiency, with encapsulation rates of 76.92%. **Conclusion:** This dual-functional scaffold addresses infection control and inflammation reduction, offering a comprehensive approach to wound management. The synergistic effect of ozenoxacin and curcumin accelerates wound healing; making it a promising candidate for advanced wound care applications.

Keywords: Electrospinning, Nanofibres, Ozenoxacin, Wound healing.

Correspondence:

Dr. Saba Maanvizhi
Professor, Department of Pharmaceutics, Sri Ramachandra Faculty of Pharmacy, Sri Ramachandra Institute of Higher Education and Research (DU), Tamil Nadu, INDIA.

Email: sabamaanvizhi@sriramachandra.edu.in

SCAN QR CODE TO VIEW ONLINE



www.ajbls.com

DOI: 10.5530/ajbls.2024.13.103

INTRODUCTION

The human skin, the largest organ in the human body, acts as a critical barrier between essential internal organs and the external environment, enabling vital functions to proceed in a controlled manner.^[1] When the skin is injured due to accidents, violence, or surgery, the resultant wound can penetrate the subcutaneous tissue and affect

other connective tissues such as tendons, muscles, nerves, parenchymal organs, arteries and even bones.^[2] This high incidence of wounds, particularly among the elderly, has a significant social and economic impact worldwide.^[3] According to a 2023 retrospective analysis by the World Health Organization, approximately 8.2 million people had at least 1 type of wound with or without infections, with treatment costs ranging from \$28.5 to \$97.0 billion. Surgical wounds incurred the highest treatment expenses, followed by diabetic foot ulcers, with outpatient wound treatment costs exceeding inpatient care costs.^[4]

Wounds vary in nature, from acute to chronic, with chronic wounds often associated with conditions like venous, arterial, diabetic and pressure ulcers, which can destroy the cutaneous covering either partially or completely.^[5] Depending on the wound's depth, it can be limited to the epidermal or dermal layers, with superficial wounds healing through regeneration, while Full-Thickness Wounds (FTWs), which extend beyond the dermis and epidermis into subdermal tissues, do not heal spontaneously due to a lack of healing cells except at the wound periphery.^[6] Wound infections, caused by microorganisms at the wound site, trigger an inflammatory response from the immune system, destroying tissue and slowing down the healing process. This issue is exacerbated in individuals with immune-suppressive conditions or autoimmune diseases such as diabetes, rheumatoid arthritis, cancer and recurrent infections.^[7] Additionally, the growing problem of microbial resistance to antimicrobials further complicates wound healing. Conventional wound care products aim to provide localized antibacterial effects, but bacterial wound infections remain a significant challenge in wound management.^[8]

Initially, gram-positive bacteria like *Streptococcus pyogenes* and *Staphylococcus aureus* dominate wound infections, but as chronic wounds develop, gram-negative bacteria such as *Escherichia coli* and *Pseudomonas aeruginosa* become prevalent. Indicators of wound infection include pus formation, increased redness, swelling, pain and fever. Traditional wound treatments often fall short due to their inability to control drug release, necessitating frequent medication applications that can lead to side effects and reduced patient compliance. Polymeric formulations, including chitosan, polyvinyl alcohol, alginate and gelatin, have shown promise as wound dressings due to their hemostatic properties and suitability for severe injuries.^[6] However, many existing dressings exhibit drawbacks such as poor mechanical properties, insufficient blood clotting ability and inadequate antimicrobial activity. This underscores the need for innovative dressing

materials. Biomaterial-based composite materials have emerged as promising candidates for wound dressings, driven by their biological basis and potential for enhanced antibacterial effects. Wound healing involves a complex process encompassing inflammation, tissue proliferation and tissue remodeling. Inflammation entails acute responses and the recruitment of macrophages, monocytes, antigens, neutrophils and cytokines to inhibit germ growth. Proliferation involves cell migration and extracellular matrix release, leading to tissue granulation and the formation of new blood vessels. Remodeling features the transition of epithelial to mesenchymal cells, wound contraction and scar tissue formation.^[8]

The healing process is influenced by various factors, both local and systemic. Local factors include oxygenation, which is crucial for cellular respiration, angiogenesis, collagen synthesis, microbial control and immune response. Systemic factors encompass age, hormones, stress, diabetes, obesity, smoking, alcohol consumption and medications. These factors can significantly hinder the healing process, making effective wound management essential.^[9]

Effective wound management requires a thorough assessment of the wound and the application of appropriate materials. Advances in biomedical research have shifted the focus from traditional cotton dressings to innovative products incorporating antimicrobial compounds and mechanical devices. The goal of wound care is to prevent inflammation, delay wound degeneration and accelerate healing by maintaining a regulated microenvironment.^[10] Given the increasing demand for advanced wound care solutions, this study explores the potential of biodegradable and biocompatible nanofibres loaded with ozenoxacin (antimicrobial) and curcumin (anti-inflammatory) to enhance wound healing. These nanofibres, produced through electrospinning, will undergo various *in vitro* characterizations to evaluate their efficacy in promoting faster wound healing.^[11] This research aims to contribute to the development of innovative, effective wound dressings that address the limitations of existing treatments.

MATERIALS AND METHODS

Drugs and chemicals

Ozenoxacin was obtained as a gift sample from Jamjoom Pharma, Saudi Arabia and Curcumin was obtained as a gift sample from Polyhedron Laboratories Pvt. Ltd., Poly vinyl alcohol (Molecular weight 1,15,000 g/mol) was purchased from Loba Chemie Pvt. Ltd., Gelatin (Molecular weight-1,15,000 Da) was purchased from

HiMedia laboratories Pvt. Ltd., Acetic acid was purchased from HiMedia laboratories Pvt. Ltd., Dimethyl sulfoxide was purchased from HiMedia laboratories Pvt. Ltd., and EDC (1-ethyl-3-(3-dimethylaminopropyl) carbodiimide hydrochloride) was Purchased from Sisco Research Laboratories.

Fabrication and evaluation of nanofibrous film

The creation of nanofiber formulations involves the utilization of two crucial elements solution and process parameters.

Solution parameters

In order to create nanofibres, the electrospinning apparatus needs an appropriate polymer solution. As the next section explains, solution concentration is essential to the fabrication of nanofibre.

Polymer concentration

Electrospinning largely depends heavily on the concentration of polymeric materials. Polymeric concentration is closely related with the viscosity of the solution. A higher concentration of polymeric material results in a more viscous polymeric solution, which hinders the ejection of polymeric droplets from the needle tip during electrospinning. Because of the surface tension-induced assembly of solvent molecules, low polymeric concentrations lead to poor fibre density and periodic bead formation. Consequently, the concentration of the solutions was adjusted appropriately for each of the 3 polymeric solutions and the optimal concentrations were determined to produce smooth, bead-free nanofibres with the highest density. In order to fabricate nanofibres, 1st and foremostly it is important to prepare the polymer solution in which the drugs have to be incorporated. In this experiment the polymer solution is prepared in 3 steps. Polyvinyl alcohol (10% w/v) in 30mL of distilled water was submerged overnight and further was stirred for 24 hr. (Solution A) Gelatin (19% w/v) was submerged in 30 mL acetic acid and was continuously stirred for 2 hr to obtain a homogeneous golden yellow-colored gelatin solution. (Solution B) After preparing the solutions A and B separately, allow them to settle overnight to remove the air bubbles from the polymer mixtures. Then solution B was injected towards solution A (in the ratio of 2:1) and simultaneously mixed well in the magnetic stirrer resulting to form a homogenous polymeric solution. Finally, a combination of ozenoxacin (300 mg) and Curcumin (20 mg) was introduced into a polymeric solution. The mixture was continuously stirred for 2 hr to achieve a solution with consistent viscosity.

Process parameters involved in electrospinning

Electrospinning was carried out in Holmarc Lab Equipment Nano Fibre Electrospinning Unit (Model No: HO-NFES-040B).

Electrospinning procedure

About 15 mL of the polymeric blend was loaded in 50 mL syringe and placed in electrospinning apparatus.

The flow rate is programmed to 2.5 mL/hr which was regulated by the in-built pump in the apparatus set up. Positive potential supply is given in the needle end (anode) and negative potential supply is given in the collector (cathode), which is located 16 cm from the syringe.

The electrospinning was carried out for 4 hr.

Voltage potential

The voltage applied during the electrospinning process is a crucial factor in determining the morphology of the fibre. A specific limit of potential is necessary to stretch the polymer and initiate the nanofabrication process. As the voltage that is used increases, there is a significant impact on the circumference of the fibre, their softness, the number of beads around and other morphological characteristics. To produce thin circumference smooth nanofibres with minimal beads, it is essential to use an optimized voltage during the nanofabrication process.

Flow rate of polymer solution

The feed rate directly influences the quantity of solution that is accessible for the electrospinning procedure. Regulating this volume is crucial as it directly affects the rate of fibre creation and the morphological features of the fibres. Achieving an ideal drop volume at the needle tip is vital for controlling these factors. Typically, a lower flow rate is advised as it allows ample time for the polarization of the polymer. Conversely, when the flow rate is extremely rapid, the polymer jet has limited time to dry before reaching the collector and experiences low stretching pressures. As a result, the development of beaded fibres with a large diameter occurs instead of smooth fibres with a small diameter.

Tip To Collector Distance (TCD)

The distance between syringe needle tip and collector has a very crucial part in the operation of electrospinning. Research has demonstrated that the separation between the collecting element and the syringe's tip can also impact the diameter and structures of the fibre. Briefly said, an excessively small distance causes the fibre to lose its ability to solidify before it reaches the collector, whereas an excessively lengthy distance causes the

spinning fibre to have a decreased affinity to reach the other end. Additionally, in order to facilitate a seamless flow of electrons, it is necessary to have an optimal potential difference and an electron sink maintained by the earthed collector, which also requires an optimal distance. Another crucial factor to consider is the evaporation of the solvent during the electrospinning process, which necessitates an optimal distance to ensure thorough drying of the fibre.

Electrospinning parameters

The electrospinning parameters used in this study include a combination of polymers, solvents and specific settings for the equipment. The polymers used are Polyvinyl Alcohol (PVA) and gelatin, which are dissolved in a mixture of acetic acid, Dimethyl Sulfoxide (DMSO) and distilled water as solvents. A DC voltage of 20 Kilovolts (KV) is applied to the system. The solution is delivered at a flow rate of 2.5 milliliters per hour (mL/hr), with the syringe needle positioned 16 centimeters (cm) away from the collector. A 24-gauge needle is attached to a 50-milliliter (mL) syringe, which is positioned at a height of 12 cm from the base. These parameters are set to optimize the electrospinning process for producing fibers with desirable properties.

Pre-formulation studies

In the pharmaceutical sector, pre-formulation studies are a crucial step in the medication development process. Prior to creating a dosage form, these studies aid in understanding the chemical and physical characteristics of a medicinal component. When creating a pharmaceutical product that is stable, safe and effective, data from Preformulation studies is vital. This may provide evidence in favour of the need for molecular modification or provide vital details for formulation design. Each drug's intrinsic chemical and physical properties were taken into account before creating a pharmaceutical formulation. This feature provides a structure for mixing drugs with other pharmaceutical ingredients to make dosage forms. Preformulation study aims to determine the kinetic rate profile, compatibility with other ingredients and physico-chemical properties of novel therapeutic chemicals in order to generate a dosage form that is beautiful, stable, effective and safe.^[12]

Physical properties of the drug and polymers

Organoleptic characters

The look, color, smell and taste of the drug ingredient are among its organoleptic attributes. Ozenoxacin and curcumin color, taste, smell and appearance were examined.^[13]

Solubility Profile of Drug

The solubility study of the drug was carried out in different solvents like water, acetic acid hexafluoro isopropanol, DMSO, polyethylene glycol, sodium lauryl sulphate+water, tween 80, ethyl acetate, chloroform, acetone, trifluoroethanol and PBS 7.4.^[14]

Construction of calibration curve in phosphate buffer Solution

Ozenoxacin (10 mg) was accurately weighed and was taken in a dry and clean 10 mL volumetric flask and the volume was made with pH 7.4 phosphate buffer up to 10 mL, to produce a stock solution (A) of 1 mg/mL. From the above stock solution (A) pipette out 1 mL using a micropipette and taken in another 10 mL volumetric flask and the volume was made up to 10 mL with phosphate buffer to produce stock (B) solution of 100 µg/mL. From the above stock (B) solution pipette out 1 mL using a micropipette and taken in another 10 mL volumetric flask and the volume was made up to 10 mL with phosphate buffer to produce stock (C) solution of 10 µg/mL. The above stock solution is scanned in 304nm using a UV spectrophotometer. Volumetric flasks holding 10 mL was used to extract individual volumes of 0.2, 0.4, 0.6, 0.8 and 1.0 from this solution. PBS was added to each flask to make the maximum capacity of 10 mL. Then the above concentration from 0.2 to 1.0 mL concentration samples were tested in UV spectrophotometer at 304 nm and the absorbance is noted and eventually a graph is plotted as concentration vs absorbance.^[15]

Melting Point

The drugs and polymers melting points were ascertained using the Microcontroller visual melting point instrument. The melting point of the medication was examined using the capillary method. Firstly, a thin-walled capillary tube was selected and 1 end was closed by tapping it on a hard surface. The open end of the capillary tube was filled with approximately 2-3 mM of the ozenoxacin sample. The powdered sample or a spatula was used to pack the sample tightly. It was ensured that the sample was compact and free of air bubbles. The microcontroller melting point apparatus was powered on and allowed to warm up. The filled capillary tube was inserted into the designed holder of the apparatus, ensuring it was positioned vertically and securely. The heating rate was adjusted to approximately 4 to 5°C for controlled heating. The temperature readings displayed were monitored and the apparatus automatically regulated the heating rate. On 1 side, a sealed capillary was tapped with a tiny sample of the medication. After the capillary was

inserted into the capillary holder, the device began to operate. The drug's melting point was visually examined and contrasted with the conventional melting point of the substance. The temperature at which the 1st signs of melting were observed (initial melting point) and when the entire sample had melted (Final melting point) were recorded. The initial and final melting points were recorded.^[16]

Fourier transform infrared spectroscopy

The IR spectrum of any compound reveals information about the functional groups present in that particular compound. IR spectrum of drug and polymers were obtained using FTIR spectrophotometer Bruker alpha 2 (Germany) and was compared with the reference standards. In order to obtain IR spectra, a small quantity of the sample was triturated with KBr preferably in the ratio of 1:100. This mixture was then compressed into a pellet which was then placed into the FTIR assembly and the IR spectrum was obtained.^[17]

X-ray crystallography

A Bruker D8 Advance X-ray diffractometer operating in the 40 kV-40 mA, 200 scanning mode and employing CuK α radiation ($\lambda=1.5406 \text{ \AA}$) was used to record the X-ray diffraction (XRD) pattern of the generated materials. Data were gathered spanning the 2θ range of 5 to 90° at a step of 0.029649°.^[18]

In vitro characterization of nanofibrous film

Viscosity

The viscosity of polymer solutions was measured at 20 rpm and 25°C with the Brookfield Viscometer II+model with spindle number S-64. Once a steady reading appeared on the viscometer, the results were recorded.^[19]

Thickness

The ability of hydrogel films to absorb humidity, surface format, swell behaviour and the deterioration behaviour in biological systems are all influenced by their thickness. Using a screw gauge, the nanofibrous sheets thickness was ascertained and took the mean of 3 separate assessments of the films.^[20]

Swelling index

To ascertain the swelling index of nanofibrous films, the gravimetric method was used. In summary, nanofibrous films were dried for a day at 40 to 45°C in a vacuum oven. After drying, the nanofibrous films were placed in an incubator at $37 \pm 0.2^\circ\text{C}$ and soaked in PBS 7.4. Films that had swollen were raised at various intervals until equilibrium was reached. The films were weighed on

a digital balance after being wiped dry on a wet filter paper to remove extra water from the surface.^[21] The following formula was used to determine the swelling index

$$\text{Swelling index} = \frac{(\text{Weight of swollen film} - \text{Initial weight of dried film})}{\text{Initial weight of dried film}} \times 100$$

Water absorption capacity

Being capable to absorb water is crucial for controlling exudate at the wound level. Knowing whether the wound bed is moist or dry may help you better understand the healing process. This is where the absorptive capacity comes in handy. A 1 x 1 cm square pre weighed film was weighed and then periodically reweighed in 10 mL of distilled water until their equilibrium state was reached.^[12]

$$\text{Percentage of water absorption} = \left(\frac{NF_w - NF_i}{NF_i} \right) \times 100$$

Where NF_i -Initial weight of nanofibrous film (mg), NF_w -Weight of nanofibrous film after immersed in water (mg).

Folding endurance

The film's flexibility, which is required for secure film placement to the wound alongside simple handling, was assessed by measuring the film's folding endurance. It was ascertained by physically folding the film up to 250 to 300 times or by folding it repeatedly at the same spot till the film breaks. The measurement of folding endurance was determined by how many times a film could be bent in the same spot without breaking.^[22]

Scanning electron microscopy studies

Ensure the stub is clean and devoid of contaminants to clean the stubs use the ethanol or IPA. Mount the sample on a stub. Gold Sputter coating: Use a conductive material to sputter coat the sample. Once this procedure is over, load the sample in the HRSEM Instrument chamber.

Anti-bacterial studies

EN 1276 Method

The stage 2 step 1 suspension test EN 1276 is used for disinfectants that are used in industrial, food, institutional and residential settings. The test assesses the product's ability to combat germs.

Test Method

Eight parts of the test product are introduced to 1 part test microorganism and 1 part interfering material in a

phase 2 step 1 suspension test. During the period of the contact time, the mixture is permitted to interact. To stop the bactericidal action, add 1 part of the mixture to eight parts neutralizer and 1 part water and let sit for 5 min. After that, the final combination is obtained and given a two-day incubation period to enable any remaining bacteria to multiply. A count is performed on the bacterial colony and compared to the initial culture size.^[23]

Drug entrapment efficiency

The drug-loaded nanofibres were dried at 40°C in a hot air oven to determine the entrapment effectiveness of the fabricated material. A nanofibre mat with dimensions of 1x1 cm² was then taken out and placed in 10 mL phosphate buffer 7.4 for a period of 2 hrs. Through UV examination of the corresponding solutions, the quantity of drug in each was determined and this amount was compared to the total amount of drug loaded during the electrospinning process of these fibers.^[24]

$$\% EE = \left[\frac{(\text{Total drug} - \text{Free drug})}{\text{Total drug}} \right] \times 100$$

In vitro drug release

The Franz diffusion cell device was used to determine the proportion of drug released by the produced nanofibres. The dissolving medium was phosphate buffer 7.4 in which a hollow glass tube was submerged. The tube was closed on 1 side with a cellophane membrane held together by elastic bands. The experiment involved adding a 1 x 1 cm² OZ film to a glass tube and running it at 50 rpm. The temperature was kept constant at 37±0.5°C. Each sample’s absorbance was measured at a maximum of 307 nm at predefined time intervals (1, 2 and up to 24 hr).^[25]

RESULTS

Preformulation studies

Organoleptic properties

The organoleptic properties for ozenoxacin have been examined. The report is tabulated below in the Table 1.

| Organoleptic characters | Ozenoxacin | Curcumin |
|-------------------------|----------------|----------|
| Colour | Off-white | Yellow |
| Odour | Characteristic | Pungent |
| Taste | Sour to bitter | Bitter |

Solubility

The solubility studies for the ozenoxacin are examined. Ozenoxacin is freely soluble in solvents like acetic acid, hexafluoro isopropanol, dimethyl sulfoxide, trifluoroethanol and partially soluble in Tween 80, ethyl acetate, chloroform, acetone, trifluoroethanol, phosphate buffer 7.4, water.

Construction of calibration curve

The calibration curve for Ozenoxacin in phosphate buffer (pH 7.4) shows a linear relationship (R²=0.9899) with the equation (y=0.1143x-0.0003). Ozenoxacin is soluble up to 1.0 µg/mL in phosphate buffer. The calibration curve of ozenoxacin is depicted in the below Figure 1.

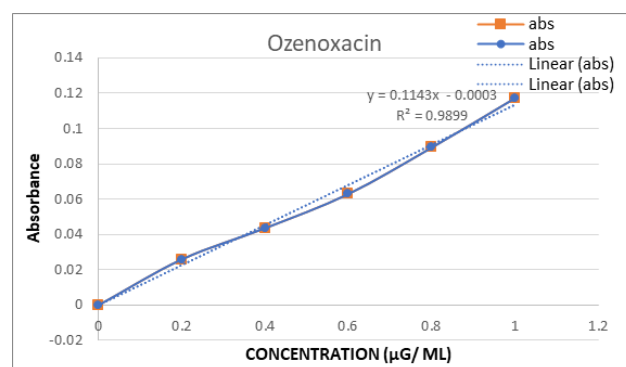


Figure 1: Calibration curve of Ozenoxacin.

Melting point

Melting points of the drugs and polymers measurement is reported in Table 2.

| Materials | Expected range | Practical value |
|------------|----------------|-----------------|
| Ozenoxacin | 255°C | 198.3°C |
| Curcumin | 183°C | 179.6°C |
| Gelatin | 31.7-34.2°C | 31°C |
| PVA | 180-200°C | 191°C |

Drug polymer compatibility

Fourier Transform Infra-Red spectroscopy

The Fourier Transform Infra-Red (FTIR) spectroscopy confirmed characteristic functional groups of the drugs and excipients used in this study. Hence the fabricated nanofibre is compatible. The FTIR reports of Ozenoxacin(OZ), Curcumin (CU), Polyvinyl Alcohol (PVA), Gelatin (GEL), Physical mixture and the formulated nanofiber (NF) is given in the Figure 2.

Ozenoxacin (OZ)

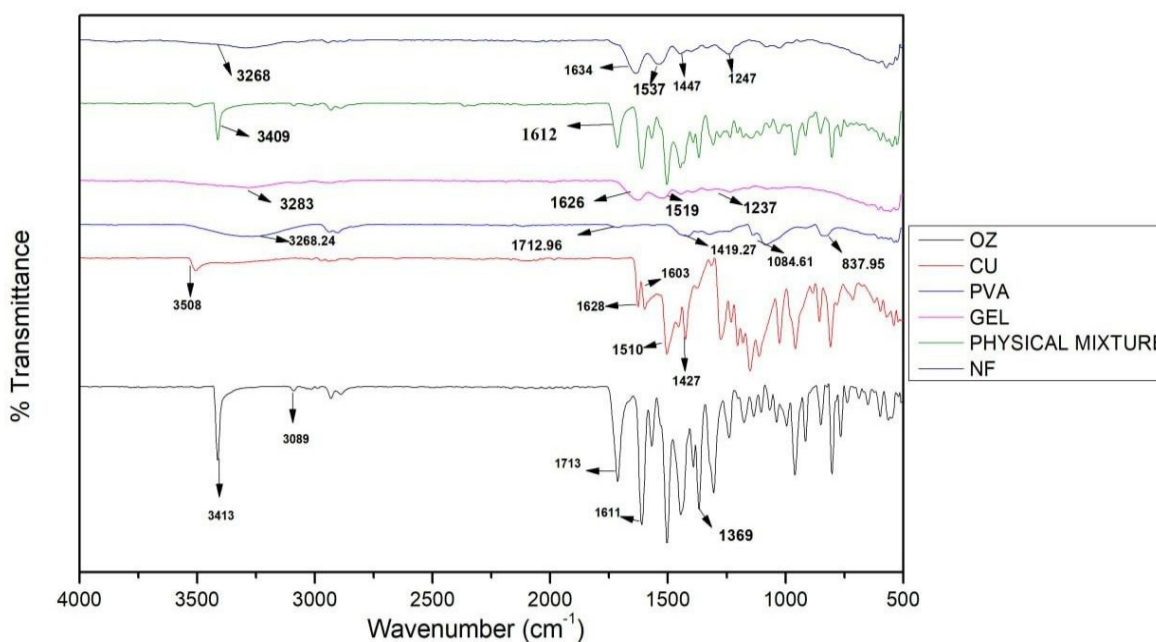


Figure 2: FTIR report (at column width).

The spectrum for ozenoxacin shows peaks around 3413 cm^{-1} and 3089 cm^{-1} , likely due to O-H and N-H stretching vibrations, respectively. Other notable peaks include 1713 cm^{-1} , which may correspond to C=O stretching and 1510 cm^{-1} , which is associated with C=C stretching in aromatic rings.

Curcumin (CU)

Curcumin displays a prominent peak at 3409 cm^{-1} for O-H stretching. The peak at 1628 cm^{-1} can be attributed to C=O stretching, while peaks at 1519 cm^{-1} and 1427 cm^{-1} indicate C=C stretching in the aromatic ring structure.

Polyvinyl Alcohol (PVA)

The PVA spectrum shows a broad O-H stretching band at 3283 cm^{-1} , indicating the presence of hydroxyl groups. The peaks at 1634 cm^{-1} and 1247 cm^{-1} are associated with C=O stretching and C-O stretching, respectively.

Gelatin (GEL)

Gelatin exhibits a strong peak at 3288 cm^{-1} , also representing O-H or N-H stretching. Peaks at 1712 cm^{-1} and 1626 cm^{-1} are typical of amide I and amide II bands, indicating the presence of proteins.

Physical Mixture

The physical mixture of ozenoxacin, curcumin, PVA and gelatin shows characteristic peaks from all components, but with some shifts indicating interactions between the functional groups. For instance, the peak at 3288 cm^{-1}

is broadened, suggesting possible hydrogen bonding among components.

Nanofiber (NF)

The nanofiber spectrum shows further shifts and broadenings in peaks, indicating enhanced molecular interactions in the nanofiber matrix. The peak at 3413 cm^{-1} is broader, suggesting stronger hydrogen bonding between hydroxyl and amide groups from PVA and gelatin, as well as ozenoxacin and curcumin. The slight shift in the C=O stretching peak from 1713 cm^{-1} to around 1711 cm^{-1} implies interactions between curcumin and ozenoxacin in the nanofiber.

Bonding Interpretations

Hydrogen Bonding

The broad peaks around $3288\text{--}3413\text{ cm}^{-1}$ across spectra indicate extensive hydrogen bonding, especially in the nanofiber, due to the presence of hydroxyl (O-H) and amide (N-H) groups in PVA, gelatin, ozenoxacin and curcumin.

Amide Bonding

The peaks around $1634\text{--}1713\text{ cm}^{-1}$ (C=O stretching) reflect the amide I and amide II bands, particularly from gelatin. These bonds are preserved in the nanofiber, though with minor shifts, indicating structural stability with some molecular interactions.

Aromatic C=C Bonds

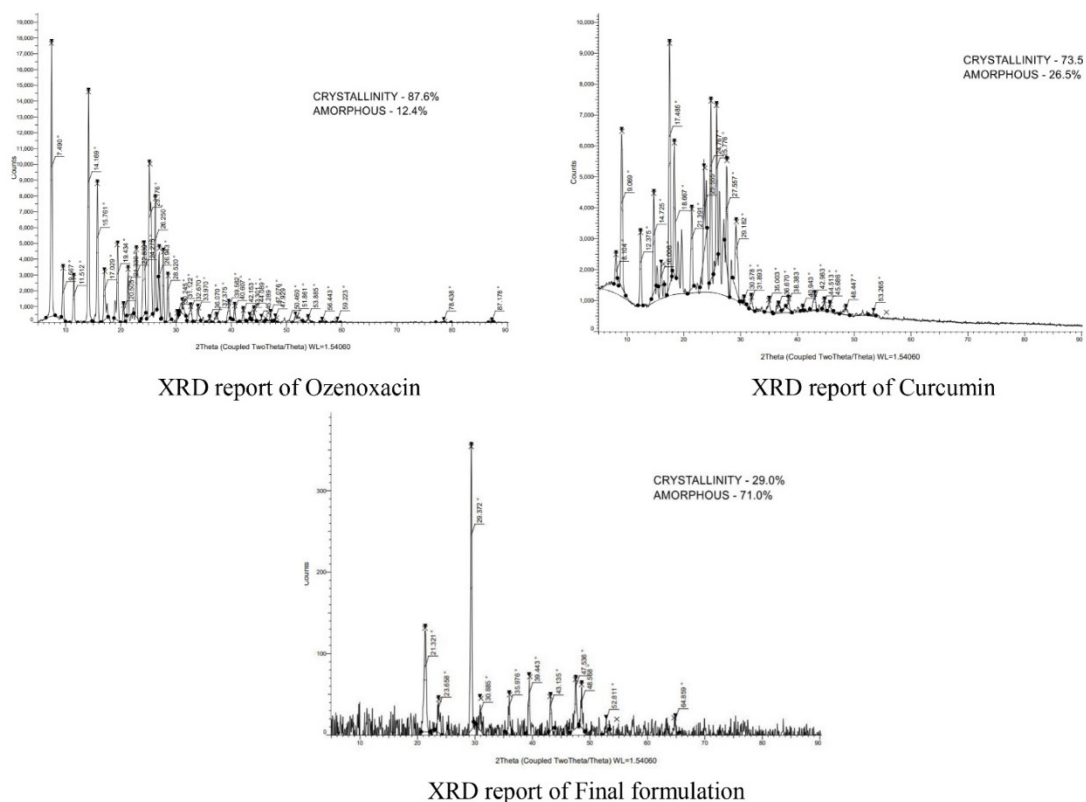


Figure 3: XRD reports of ozenoxacin, Curcumin and final formulation.

Peaks around $1510\text{--}1603\text{ cm}^{-1}$ correspond to aromatic C=C stretching in curcumin and ozenoxacin. The retention of these peaks suggests that the aromatic structure remains intact in the nanofiber.

XRD studies

XRD patterns reveal the compound's nature—whether crystalline or amorphous, as well as certain structural traits of the crystalline form. Figure 3 displays the X-ray diffraction (XRD) pattern of (a) Ozenoxacin, (b) Curcumin and (c) Fabricated drug loaded nanofibre.

A-Ozenoxacin

The X-ray Diffraction (XRD) analysis of Ozenoxacin reveals a crystallinity of 87.6% and an amorphous content of 12.4%. Significant diffraction peaks are observed at 2θ values of 7.490° , 11.512° , 14.169° , 15.76° and others, indicating the crystalline structure of the compound. The high degree of crystallinity suggests a well-defined structure, while the minor amorphous content indicates some regions lacking long-range order. This structural information is crucial for understanding the physical properties of Ozenoxacin, which is important for its formulation and application in the pharmaceutical industry.

B-Curcumin

The X-ray Diffraction (XRD) analysis of Curcumin reveals a crystallinity of 73.5% and an amorphous content of 26.5%. Significant diffraction peaks are observed at 2θ values of 8.098° , 11.276° , 14.725° , 17.465° , 23.187° and 27.557° , indicating the crystalline structure of the compound. The moderate degree of crystallinity suggests a substantial well-defined structure, while the higher amorphous content indicates notable regions lacking long-range order. This structural information is crucial for understanding the physical properties of Curcumin, influencing its solubility, bioavailability and stability in pharmaceutical applications.

C-Fabricated drug loaded nanofibre

The X-ray diffraction (XRD) analysis of nanofibres formulated with Polyvinyl Alcohol (PVA), gelatin, Ozenoxacin and Curcumin reveals a crystallinity of 29.0% and an amorphous content of 71.0%. Significant diffraction peaks are observed at 2θ values of 12.321° , 23.659° , 29.372° , 30.865° , 39.616° , 43.135° , 53.443° , 55.976° and 64.899° , indicating crystalline regions within the nanofibre sample. The high amorphous content suggests a predominantly disordered structure, typical for polymer-based nanofibres, where the polymers contribute to the amorphous nature, while the APIs (Ozenoxacin and curcumin) introduce crystalline

characteristics. This balance between crystalline and amorphous phases affects the mechanical properties, drug release rates and stability of the nanofibres, crucial for optimizing pharmaceutical applications. The XRD pattern displayed in the Figure above shows the intensity of diffracted X-rays as a function of 2 theta, providing detailed insight into the structural composition of the nanofibres.

In vitro characterization of nanofibrous film

Mechanical properties of the fabricated nanofibrous film

Viscosity

The viscosity of the polymer solution was evaluated through the Brookfield Viscometer II model, with spindle number S-64. The viscosity of the polymer solution was found to be 39.48 Pa s.

Swelling index nanofibrous film

The swelling index of the drug-loaded nanofibrous film was ascertained. The swelling index of the drug-loaded nanofibre was found to be 163.

Drug entrapment efficiency

The entrapment efficiency of the drug-loaded nanofibres was examined. The entrapment efficacy of the drug-loaded fabricated nanofibres was found to be 76.92%.

Folding endurance

The nanofibres formulated with PVA, gelatin, Ozenoxacin and Curcumin exhibit a folding endurance value of 93, indicating strong mechanical properties and high flexibility. These characteristics are essential for ensuring the durability and reliability of the nanofibres in various pharmaceutical applications.

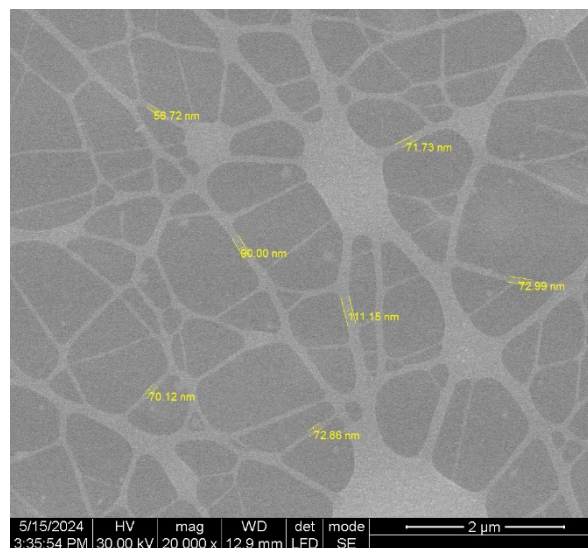
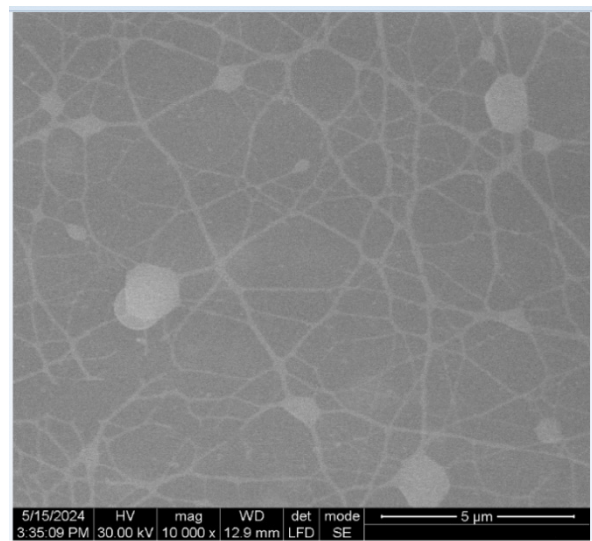
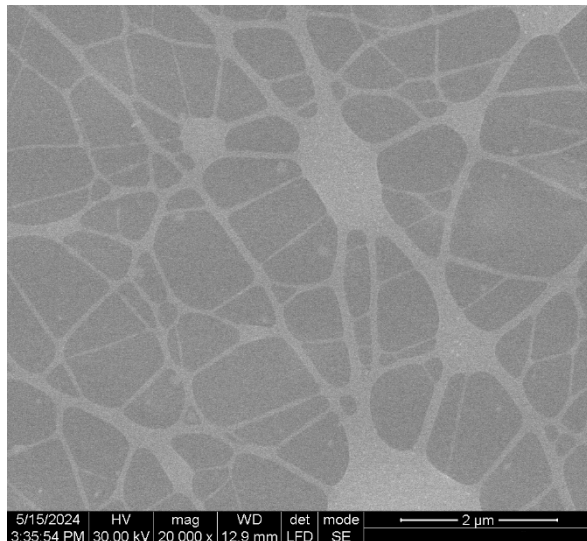

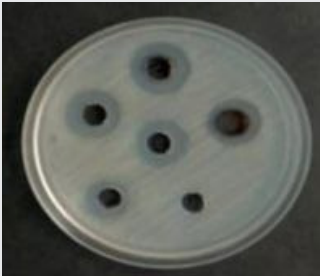


Figure 4: Sem images of formulated drug loaded nanofibers.

Table 3: Anti-bacterial activity.

| Sl. No. | Test Organism | Initial Microbial Count (CFU/mL) | Initial Count Log 10 | Last Count (cfu/mL) | Last Count Log Reduction | Limit | Anti-bacterial Efficacy % |
|---------|--|----------------------------------|----------------------|---------------------|--------------------------|-------|---------------------------|
| 1. |  <i>Candida albicans</i> | 2332748 | 6.129 | 2432 | 3.31 | >4 | 99.886 |
| 2. |  <i>Streptococcus aureus</i> | 2218009 | 6.930 | 2679 | 2.89 | >4 | 99.326 |

Scanning Electron Microscopy (SEM)

The surface morphology of the optimized formulation was investigated using Scanning Electron Microscopy. The SEM analysis of PVA and gelatin nanofibres loaded with Ozenoxacin and Curcumin, captured at 30.00 kV and magnifications of 10,000x and 20,000x, reveals a well-formed network. The nanofibres exhibit a smooth structure with uniform diameters and lengths, measuring approximately 50.67 nm to 114.40 nm and show no signs of agglomerations. The Figure 4 illustrate fibre morphology with consistent and interconnected fibre morphology essential for mechanical integrity and effective drug delivery. Spherical particles observed suggest successful loading of the active compounds. This uniformity and smoothness in the nanofibres are crucial for controlled release applications. Additionally, *in vitro* release studies have been conducted to understand the drug release profile. The SEM images confirm that the nanofibres are well-distributed, with consistent morphology, making them suitable for therapeutic use.

Anti-bacterial study

The antibacterial study for the developed nanofibres was performed. The results are tabulated below in the Table 3.

The fabricated nanofibres were tested for antibacterial efficacy against *Candida albicans* and *Streptococcus aureus*. The initial microbial count for *Candida albicans* was 2,332,748 CFU/mL, which reduced to 2,432 CFU/mL,

demonstrating a log reduction of 3.31 and an efficacy of 99.886%. For *S. aureus*, the initial count was 2,218,009 CFU/mL, reducing to 2,679 CFU/mL, indicating a log reduction of 2.89 and an efficacy of 99.326%. Both results exceed the limit of a 4-log reduction, proving the nanofibres' significant antibacterial properties against these pathogens.

In vitro drug release

Several computational models, including the zero order, first order, Peppas and Higuchi models, were used to comprehend the drug release process from the developed formulations. The potential drug release mechanism was described by the model with the highest R² value, which is regarded as the best fit model.

The Korsmeyer-Peppas model, with the highest R² value of 0.992, is the best fit for the release kinetics of the nanofibres. This indicates that the release mechanism is likely a combination of diffusion and erosion, characteristic of the Korsmeyer-Peppas model. Additionally, the First-order model, with an R² value of 0.9842, also closely follows the release kinetics. The analysis shows that the release kinetics of the nanofibres follows both the Korsmeyer-Peppas and First-order models, with the Korsmeyer-Peppas model providing the best fit. Both models indicate sustained release, making the nanofibres suitable for applications requiring controlled and prolonged drug delivery. The fitted curves and the relevant equations are described in Figure 5.

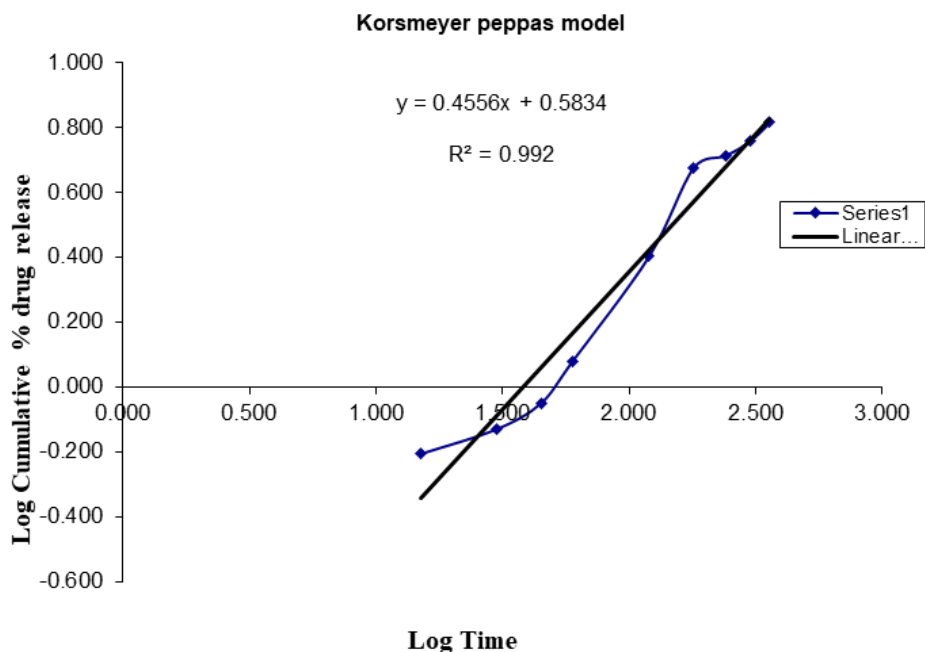


Figure 5: Korsmeyer peppas model.

DISCUSSION

In the pre-formulation studies, the organoleptic studies ensure the identification of the drug and its acceptability in formulations. Observing specific physical properties helps in initial quality assessments. Melting point data helped in judgement of the drug and polymers and also to assess its purity. It also determines the compatibility with polymers and excipients during formulation processes. FTIR analysis ensures that there are no incompatibilities among the drug and polymers used in this present study. The shifts in characteristic peaks suggest hydrogen bonding and other interactions is crucial for forming a stable nanofibre system. XRD analysis demonstrates that reduced crystallinity in nanofibres indicates improved solubility and regulated release of the medication. Drug delivery performance is optimized by controlling the mechanical characteristics and release profiles of the nanofibres through an equilibrium between crystalline and amorphous phases.

The viscosity of the polymer solution prior to electrospinning was found to be at 39.48 Pa.s, ensuring optimal fibre formation. The high swelling capacity reflects better drug retention and release potential, improving the film's performance in pharmaceutical applications. The high drug entrapment ensures minimal drug wastage and uniform drug distribution in the nanofibres, which is critical parameter for sustained release applications. Folding endurance of the fabricated nanofibres was found to be 93, which confirms that the fabricated nanofibres through electrospinning process has strong mechanical properties with high flexibility

ensure durability and reliability of the nanofibres during handling and use. Scanning Electron Microscopy (SEM) confirmed uniform fibres with diameters between 50-114 nm, which is essential for controlled drug release. Smooth and uniform nanofibres ensure mechanical integrity and proper drug distribution throughout the fabricated nanofibres. The high antibacterial efficacy indicates the nanofibres potential for treating infections caused by the pathogens. Their significant reduction in microbial counts supports their use in targeted applications. The release kinetics confirms sustained drug release, essential for applications requiring prolonged therapeutic effects. Korsmeyer-Peppas fitting suggests the combination of diffusion and matrix erosion mechanisms in drug release. The controlled drug release profile, modeled effectively using the Korsmeyer-Peppas model ($R^2=0.992$), confirmed a sustained therapeutic effect that aligns with previous studies utilizing similar controlled-release systems. For instance, while previous studies by Fahimirad *et al.* (2021) and Mahmud *et al.* (2020) achieved improved wound healing and controlled curcumin release, this research's dual-agent formulation demonstrated superior antibacterial efficiency and release control.^[26]

The developed nanofiber demonstrates a range of compelling strengths that position it as a promising solution for advanced wound healing applications. Through rigorous characterization, the nanofiber's physical, mechanical and antibacterial properties have been meticulously evaluated, ensuring its suitability for the complex demands of wound care. The integration of dual therapeutic agents, ozenoxacin and curcumin, adds significant value to its functionality by combining potent

antibacterial and anti-inflammatory actions. Ozenoxacin effectively addresses bacterial infections, a common complication in wound healing, while curcumin's well-documented anti-inflammatory properties aid in reducing inflammation and promoting tissue regeneration. This dual-action synergy provides a comprehensive approach to wound management, targeting both microbial control and the inflammatory cascade.

An additional strength of this nanofiber lies in its controlled drug release profile, which has been validated through predictive modeling. The sustained release of both therapeutic agents ensures prolonged therapeutic action, reducing the need for frequent dressing changes a critical factor for enhancing patient comfort and compliance. Such a controlled release mechanism not only minimizes the risk of drug wastage but also ensures that optimal concentrations of the agents are maintained at the wound site over an extended period, fostering a more efficient healing process. The mechanical robustness of the nanofiber further enhances its practicality as a wound dressing, providing the necessary structural integrity to withstand handling during application and ensuring durability throughout the treatment period.

However, a notable limitation of this study is the absence of *in vivo* testing, which limits the ability to assess the material's real-world performance in clinical scenarios. While the *in vitro* characterizations provide valuable insights into the nanofiber's properties and functionality, the lack of animal or human trials leads to constraint about its biocompatibility, long-term safety and effectiveness unanswered. Bridging this gap will require further research involving *in vivo* and clinical evaluations to validate its therapeutic potential and address the complexities of dynamic wound environments.

Despite this limitation, the findings of the study carry significant implications for both practical applications and future research. The nanofiber emerges as a highly promising wound dressing material with a unique combination of improved mechanical properties, a dual therapeutic approach and a controlled drug release system. Its potential to reduce the frequency of treatments and improve healing outcomes presents an opportunity for transforming conventional wound care practices. Moreover, this research lays the groundwork for advancing the field of multi-agent nanofibers, emphasizing the need for more in-depth *in vivo* and clinical trials to establish their clinical viability. These efforts could ultimately lead to the adoption of such innovative materials in real-world healthcare settings, offering a novel solution to the persistent challenges of wound healing.

CONCLUSION

This research work had successfully developed biodegradable and biocompatible nanofibers using Polyvinyl Alcohol (PVA) and gelatin, loaded with ozenoxacin and curcumin for enhanced wound healing. These nanofibers exhibited optimal physical, mechanical and biological properties, including smooth and uniform structure, excellent mechanical strength, significant water absorption capacity, high drug entrapment efficiency, substantial antibacterial activity and sustained drug release profiles. The present study demonstrated that the nanofibers could effectively promote wound healing by providing antimicrobial protection, reducing inflammation and facilitating sustained drug release. Future research should focus on *in vivo* studies to validate efficacy and safety in clinical settings, explore enhanced formulations with additional bioactive compounds and develop personalized wound dressings tailored to specific needs. Investigating the long-term stability and storage conditions, scaling up production and exploring new biodegradable materials are also crucial for practical application and commercialization. This innovative approach offers significant potential for improving patient outcomes and reducing healthcare costs associated with wound management.

ACKNOWLEDGEMENT

The authors would like to acknowledge the higher official's and management of Sri Ramachandra Institute of Higher Education and Research (DU), Chennai, India.

CONFLICT OF INTEREST

The authors declare that there is no conflict of interest.

ABBREVIATIONS

PVA: Polyvinyl Alcohol; **SEM:** Scanning Electron Microscopy; **FTIR:** Fourier Transform Infra-Red Spectroscopy; **XRD:** X-ray Diffraction; **FTW:** Full Thickness Wounds; **TCD:** Tip to Collector Distance; **CFU:** Colony Forming Unit.

SUMMARY

This study highlights the potential of dual-drug-loaded nanofibers as innovative wound dressing materials. The combination of strong mechanical properties, controlled drug release and dual therapeutic action provides a comprehensive solution for chronic wound care. These findings pave the way for future *in vivo*

and clinical evaluations, with the goal of translating this technology into practical, real-world applications, potentially transforming modern wound management practices.

REFERENCES

- Bertram U, Steiner D, Poppitz B, Dippold D, Köhn K, Beier JP, Detsch R, Boccaccini AR, Schubert DW, Horch RE AA. Vascular Tissue Engineering: Effects of Integrating Collagen into a PCL Based Nanofiber Material. *Biomed Research International*. 2017;2017:1-11.
- Tamer T.M., Sabet M.M. *et al.* Hemostatic and antibacterial PVA/Kaolin composite sponges loaded with penicillin-streptomycin for wound dressing applications. *Sci Rep*. 2021;11:1-15.
- Taheri P., Jahanmardi R. *et al.* Physical, mechanical and wound healing properties of chitosan/gelatin blend films containing tannic acid and/or bacterial nanocellulose. *Int J Biol Macromol*. 2020;154:421-32.
- Spampinato S.F., CGI *et al.* The treatment of impaired wound healing in diabetes, looking among old drugs. *Nanomaterials*. 2020;13:60.
- Moore A.L., Marshall C.D *et al.* Scarless wound healing, transitioning from fetal research to regenerative healing. *Wiley Interdisciplinary Reviews. Dev Biol*. 2018;7:309-18.
- Sharma A., Puri V. *et al.* Rifampicin-Loaded Alginate-Gelatin Fibers Incorporated within Transdermal Films as a Fiber-in-Film System for Wound Healing Applications. *Membranes (Basel)*. 2021;11:7-14.
- Chan LK, Withey S BP (2006). Smoking and wound healing prob_lems in reduction mammoplasty: is the introduction of urine nicotine testing justified. *Plast Surg*. 2006;56:111-5.
- Sharma A., Puri V. *et al.* (2020). Biopolymeric, nanopatterned, fibrous carriers for wound healing applications. *Curr Pharm Des*. 2020;26:4894-908.
- Shi Y, Wei Z, Zhao H, Liu T, Dong A, Zhang J. Electrospinning of ibuprofen-loaded composite nanofibers for improving the performances of transdermal patches. *J Nanosci Nanotechnol*. 2013;13(6):3855-63.
- Rea S, Giles NL, Webb S, Adcroft KF, Evill LM, Strickland DH *et al.* Bone marrow-derived cells in the healing burn wound—more than just inflammation. *Biomacromolecules*. 2015;35:356-64.
- Kirchner LM, Meerbaum SO, Gruber BS, Knoll AK, Bulgrin J TR, Al. E. Effects of vascular endothelial growth factor on wound closure rates in the genetically diabetic mouse model. *wound repair Regen*. 2003;11:127-31.
- Dias J.R., Baptista-Silva S. *et al.* In situ crosslinked electrospun gelatin nanofibers for skin regeneration. *Eur Polym J*. 2017;95:161-73.
- Zahiri M., Khanmohammadi M. *et al.* Encapsulation of curcumin loaded chitosan nanoparticle within poly (ϵ -caprolactone) and gelatin fiber mat for wound healing and layered dermal reconstitution. *Int J Biol Macromol*. 2019;153:1241-50.
- Zhang D., Li L. *et al.* *in vivo* study of silk fibroin/gelatin electrospun nanofiber dressing loaded with astragaloside IV on the effect of promoting wound healing and relieving sca. *J Drug Deliv Sci Technol*. 2019;52:272-81.
- Najafiasl M., Osfouri S. *et al.* Alginate-based electrospun core/shell nanofibers containing dexamphenol, A good candidate for wound dressing. *J Drug Deliv Sci Technol*. 2020;57:101708.
- Esmaeili E., Eslami-Arshaghi T. *et al.* The biomedical potential of cellulose acetate/polyurethane nanofibrous mats containing reduced graphene oxide/silver nanocomposites and curcumin, Antimicrobial performance and cutaneous wound healin. *Int J Biol Macromol*. 2020;152:418-27.
- Elakkiya T., Malarvizhi G. *et al.* Curcumin loaded electrospun bombyx mori silk nanofibers for drug delivery. *Polym Int*. 2014;63:100-5.
- El-Aassar M. R., Ibrahim O. M. *et al.* Wound dressing of chitosan-based-crosslinked gelatin/polyvinyl pyrrolidone embedded silver nanoparticles, for targeting multidrug resistance microbes. *Carbohydr Polym*. 2021;355:117484.
- Ehterami A., Salehi M. *et al.* Chitosan/alginate hydrogels containing Alpha-tocopherol for wound healing in rat model. *J Drug Deliv Sci Technol*. 2019;51:204-13.
- Manuja A., Raguvaran R. *et al.* Accelerated healing of full thickness excised skin wound in rabbits using single application of alginate/acacia based nanocomposites of ZnO nanoparticles. *Int J Biol Macromol*. 2020;155:823-33.
- Luz P.P., Silva M.L. *et al.* Curcumin-loaded biodegradable electrospun fibers, preparation, characterization and differences in fiber morphology. *Int J Polym Anal Charact*. 2014;18:534-44.
- Sundaramurthi, D.; Vasanthan, K. S.; Kuppan, P.; Krishnan, U. M.; Sethuraman S. Electrospun nanostructured chitosan-poly(vinyl alcohol) scaffolds: A biomimetic extracellular matrix as dermal substitute". *Biomed Mater*.
- Kuppan, P.; Vasanthan, K. S.; Sundaramurthi, D.; Krishnan, U. M.; Sethuraman S. "Development of poly(3-hydroxybutyrate-co-3-hydroxyvalerate) fibers for skin tissue engineer_ing: Effects of topography, mechanical and chemical stimuli." *Biomacromolecules*. 2011;12:3156-65.
- Niranjana R., Kaushik M. *et al.* Enhanced wound healing by PVA/Chitosan/ Curcumin patches, *In vitro* and *in vivo* study. *Colloids Surfaces B Biointerfaces*. 2020;182:1-8.
- Duan Y., Li K. *et al.* Preparation and evaluation of curcumin grafted hyaluronic acid modified pullulan polymers as a functional wound dressing material. *Carbohydr Polym*. 2020;238:116195.
- Fahimirad S, Abtahi H, Satei P, Ghaznavi-Rad E, Moslehi M, Ganji A. Wound healing performance of PCL/chitosan based electrospun nanofiber electrospayed with curcumin loaded chitosan nanoparticles. *Carbohydrate Polymers [Internet]*. 2021;259(October 2020):117640:5-10 Available from: <https://doi.org/10.1016/j.carbpol.2021.117640>

Cite this article: Vasanth A, Subashini P, Jerad Suresh A, Mubeena S, Alan Mathew Punnoose, Saba Maanvizhi, Fabrication and Characterization of Ozenoxacin and Curcumin Loaded Electrospun Nanofibre Membrane for Full Thickness Wound Healing: *In vitro* Assessments. *Asian J Biol Life Sci*. 2024;13(3):860-72.